

Communication

# Eight-Channel LAN WDM (De)Multiplexer Based on Cascaded Mach–Zehnder Interferometer on SOI for 400GbE

Zhizun Zhao <sup>1,2</sup> , Zhen Li <sup>1,2</sup>, Jiaqi Niu <sup>1,2</sup>, Gaolu Zhang <sup>1,2</sup>, Hongliang Chen <sup>1,2</sup>, Xin Fu <sup>1</sup> and Lin Yang <sup>1,\*</sup>

<sup>1</sup> State Key Laboratory on Integrated Optoelectronics, Institute of Semiconductors, Chinese Academy of Sciences, Beijing 100083, China; zhunzhao@semi.ac.cn (Z.Z.); lizhen2019@semi.ac.cn (Z.L.); jiaqiniu@semi.ac.cn (J.N.); zhanggaolu17@semi.ac.cn (G.Z.); chen hongliang@semi.ac.cn (H.C.); fuxin@semi.ac.cn (X.F.)

<sup>2</sup> College of Materials Science and Opto-Electronic Technology, University of Chinese Academy of Sciences, Beijing 100083, China

\* Correspondence: oip@semi.ac.cn

**Abstract:** In this paper, we design and experimentally demonstrate an eight-channel cascaded Mach–Zehnder interferometer (MZI) based Local Area Network (LAN) Wavelength Division Multiplexing (WDM) (de)multiplexer with channel spacing of 800 GHz on a silicon-on-insulator. By cascading a three-stage MZI, eight target wavelengths are (de)multiplexed. The length difference of the third-stage MZI delay arms is adjusted so that the output channels skip the guard band. In order to keep the central wavelength of each channel from shifting, we utilize a wide waveguide for the phase delay arm in MZI to achieve large fabrication tolerance, and the multi-mode interference (MMI) couplers as power splitters with weak dispersions. The measurement results of the fabricated device show the precise wavelength alignment over the whole working wavelength range.

**Keywords:** Local Area Network; Wavelength Division Multiplexing; cascaded Mach–Zehnder interferometer



**Citation:** Zhao, Z.; Li, Z.; Niu, J.; Zhang, G.; Chen, H.; Fu, X.; Yang, L. Eight-Channel LAN WDM (De)Multiplexer Based on Cascaded Mach–Zehnder Interferometer on SOI for 400GbE. *Photonics* **2022**, *9*, 252. <https://doi.org/10.3390/photonics9040252>

Received: 23 March 2022

Accepted: 9 April 2022

Published: 11 April 2022

**Publisher's Note:** MDPI stays neutral with regard to jurisdictional claims in published maps and institutional affiliations.



**Copyright:** © 2022 by the authors. Licensee MDPI, Basel, Switzerland. This article is an open access article distributed under the terms and conditions of the Creative Commons Attribution (CC BY) license (<https://creativecommons.org/licenses/by/4.0/>).

## 1. Introduction

Wavelength Division Multiplexing (WDM) is an effective means of improving communication capacity in a limited physical channel, and has been widely adopted in optical communication systems [1]. Local Area Network (LAN) WDM technology with a channel spacing of 800 GHz in the O-band is attractive for inter-data-center application due to their large capacity and long transmission distance. Among several standards for 400 Gbit/s Ethernet (400 GbE) standardized in 2017, 400GBASE-FR8 and -LR8 use the channel corresponding to the LAN WDM [2].

An optical WDM (de)multiplexer can be realized by using different device structures, such as arrayed-waveguide grating (AWG) [3,4], echelle diffraction grating (EDG) [5], or a cascaded Mach–Zehnder interferometer (MZI) [6–8]. Compared to other types of devices, the cascaded MZI has advantages in terms of low insertion loss, spectral flatness, and low crosstalk. At present, most of the research and demonstration of O-band WDM devices focuses on the cascaded MZI coarse WDM (CWDM) [9–13]. However, there are few reports on LAN WDM devices [10,14–16]. In [14], an O-band four-channel (de)multiplexer with low thermal sensitivity for a LAN WDM system is demonstrated experimentally by utilizing silicon nitride (SiN) optical waveguides. In [16], two 4-channel polarization MUXs for 1.28 and 1.3  $\mu\text{m}$  bands are designed. The MUX has  $2 \times 2$  and  $2 \times 1$  MZIs for the first 3200 GHz filters, and is connected by an on-chip polarization splitter rotator (PSR) and a TE1-TM0 mode converter. A tolerance analysis shows that the proposed MUX is robust to the change in waveguide width occurring in the fabrication process.

Because of the narrower channel spacing than CWDM (4.45 nm for LAN WDM to 20 nm for CWDM), it is more difficult to achieve the controllability of the peak wavelength

position for LAN WDM. Therefore, for 400GBASE-FR8 and -LR8, a fabrication-tolerant MUX with accurate alignment of the wavelength position is highly desired. In this article, we present an 8-channel LAN WDM (de)multiplexer for 400GbE by utilizing three-stage cascaded MZIs. In order to achieve a small size to integrate other devices, we only used a single MZI structure at each stage. The delay arms of each MZI are widened to obtain large fabrication tolerances. The power splitters use the multi-mode interference (MMI) couplers because they are wavelength-insensitive. In this way, an 8-channel LAN WDM (de)multiplexer is manufactured and experimentally demonstrated.

### 2. Design and Fabrication

The cascaded Mach–Zehnder (de)multiplexer is based on a series of four-port lattice filter building blocks serving as wavelength splitters. To implement an 8-channel LAN WDM, three filter stages with different free spectral ranges and different central wavelengths are connected in a binary tree configuration [17,18]. Figure 1a shows the schematic diagram of the presented 8-channel (de)multiplexer and the demultiplexing process, and the central wavelength and range of eight channels specified in 400 GbE is shown in Table 1. The 8 input wavelength bands are divided into two groups by each MZI filter, and eventually demultiplexed to a dedicated output port.

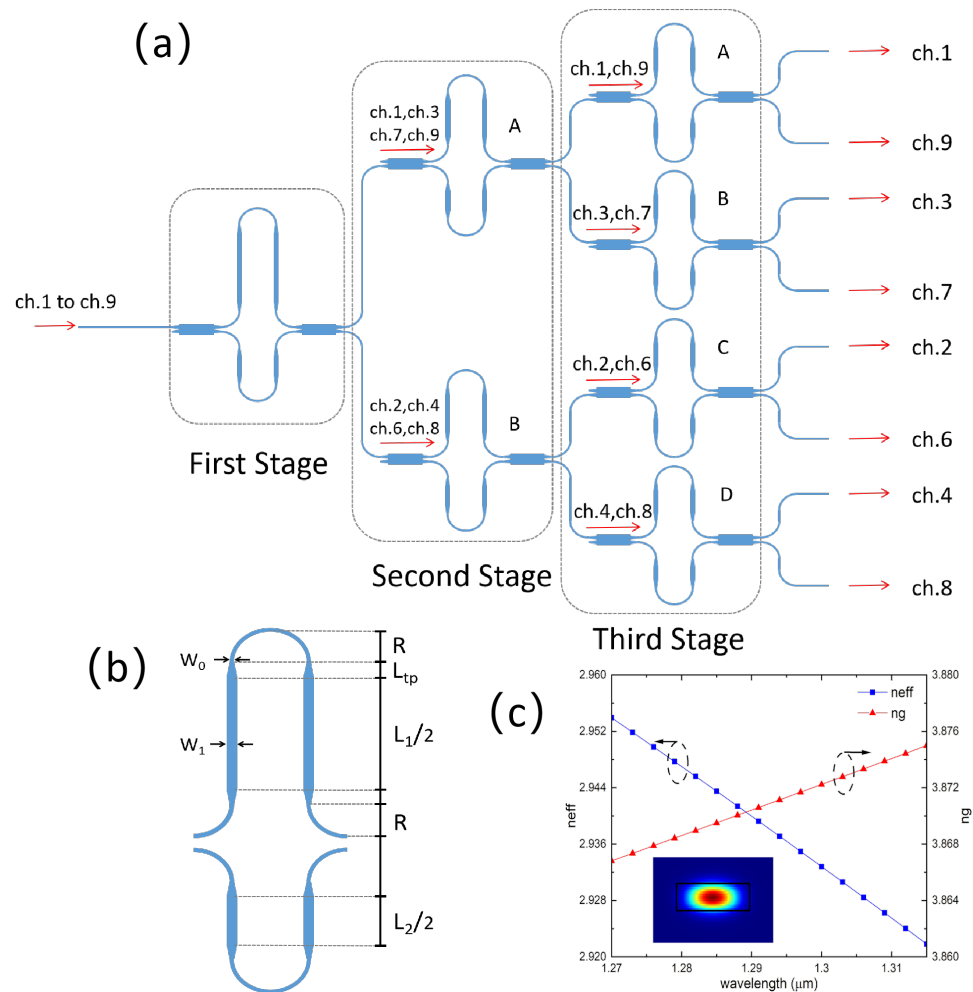


**Figure 1.** Schematic diagram of (a) the 8-channel (de)multiplexer and the demultiplexing process and (b) the delay arms in MZI.  $W_0 = 0.41 \mu\text{m}$ ,  $W_1 = 1 \mu\text{m}$ ,  $L_{tp} = 5 \mu\text{m}$ ,  $R = 10 \mu\text{m}$ . (c) The simulation result of the waveguide effective index and group index from 1270 nm to 1315 nm wavelength range. Group index is given by  $n_g = n_{eff}(\lambda) - \lambda \frac{dn_{eff}}{d\lambda}$ .

**Table 1.** The central wavelength and range of eight channels.

Lane	Ch1	Ch2	Ch3	Ch4
Wavelength (nm)	1273.5	1277.9	1282.3	1286.7
Span (nm)	1272.55–1274.54	1276.89–1278.89	1281.25–1283.27	1258.65–1287.68
Lane	Ch6	Ch7	Ch8	Ch9
Wavelength (nm)	1295.6	1300.1	1304.6	1309.1
Span (nm)	1294.53–1296.59	1299.02–1301.09	1303.54–1305.63	1308.09–1310.19

A single MZI is composed of two couplers and two delay arms. The design of the length difference between two arms is the key of the device, which is related to the change of phase. It will affect both the free spectral region and central wavelength of the MZI. The waveguide-width deviation caused by fabrication errors is a significant factor of phase error. In order to inhibit the negative effect, a 1- $\mu\text{m}$ -wide waveguide is used in the straight waveguide portion of the delay arms [13,19]. All bent waveguides' widths are chosen to be  $W_0 = 0.41 \mu\text{m}$  and they are connected to the wide waveguides using identical linear tapers with a length of 5  $\mu\text{m}$  to ensure only  $\text{TE}_0$  mode propagation, as shown in Figure 1b.

We firstly calculate the waveguide effective index ( $n_{eff}$ ) and group index ( $n_g$ ) from 1270 nm to 1315 nm wavelength by using the finite-difference eigenmode (FDE) method (Lumerical MODE). Here, we primarily consider the fundamental TE mode ( $\text{TE}_0$ ). The waveguide is built on an SOI platform with a 220-nm-thick top silicon layer and a 2000-nm-thick buried oxide layer. The upper cladding is a 3000-nm-thick oxide thin film. Figure 1c shows the simulation result. We then calculate the length difference between two arms ( $\Delta L$ ) of each MZI. The 1st-stage MZI needs an FSR equal to two times the channel spacing (4.5 nm) to separate 8-wavelength light into two groups, and the value of the length difference is given by [7]:

$$\Delta L_1 = \frac{\lambda^2}{2 \cdot \delta\lambda \cdot n_g} \tag{1}$$

Then, the 2nd-stage (3rd-stage) MZI continues to separate the wavelength channels with an FSR equal to four (eight) times the channel spacing. Therefore, the length difference between two arms is  $\Delta L_1/2$  of the 2nd-stage MZI and  $\Delta L_1/4$  of the 3rd-stage MZI similarly. Since 1291 nm is not in the channel wavelength range required for the LAN WDM, the FSR of the 3rd-stage MZI that filters the 1st and 8th channels should be sixteen times the channel spacing, and the length difference is  $\Delta L_1/8$ , to skip this wavelength range. Finally, we adjust the wavelength position of the pass bands. These should be moved by a fraction of one FSR to separate channels. A shift of one full FSR is achieved by adding a delay arm length difference of [7]:

$$\Delta L_{shift} = \frac{\lambda}{n_{eff}} \tag{2}$$

The correct setting and total length of the arm length difference for all MZIs are summarized in Table 2.

**Table 2.** Parameters for the calculation of the delay line lengths.

MZIs	$\Delta L$	Total Length ( $\mu\text{m}$ )
1st	$\Delta L_1$	48.4
2st_A	$\Delta L_1/2$	24.2
2st_B	$\Delta L_1/2 + 0.75\Delta L_{shift}$	24.53
3rd_A	$\Delta L_1/8$	6.05
3rd_B	$\Delta L_1/4 + 0.25\Delta L_{shift}$	12.21
3rd_C	$\Delta L_1/4 + 0.125\Delta L_{shift}$	12.156
3rd_D	$\Delta L_1/4 + 0.375\Delta L_{shift}$	12.264

A broadband coupler is another important issue in this design. All the splitters of MZIs are based on  $2 \times 2$  multi-mode interference (MMI) couplers with a 50:50 splitting

ratio [9]. We optimize the MMI parameters by using the eigenmode expansion (EME) method (Lumerical MODE). The simulation structure model is shown in Figure 2 and the parameters are chosen to be as follows:  $L_{MMI} = 54.2 \mu\text{m}$ ,  $W_{MMI} = 6 \mu\text{m}$ ,  $L_{taper} = 12 \mu\text{m}$  and  $W_{taper} = 1.8 \mu\text{m}$ .

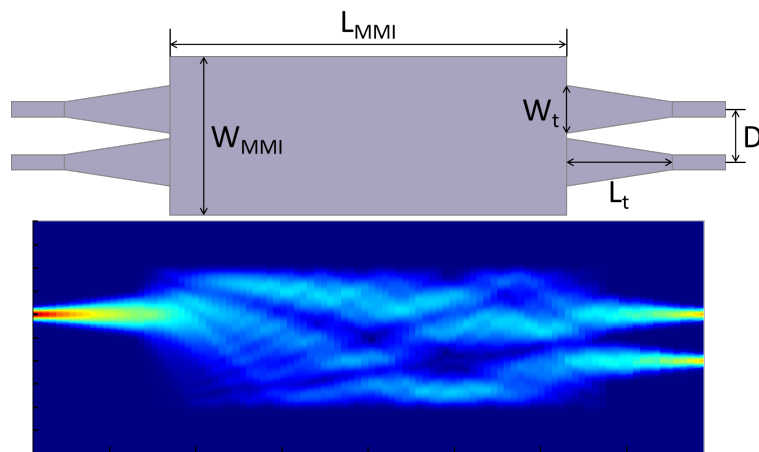


Figure 2. Schematic diagram of  $2 \times 2$  MMI and the simulation result of mode field distribution.

To verify the feasibility of the design, we utilize an optical circuit solver (Lumerical INTERCONNECT) to construct an 8-channel cascaded MZI-type (de)multiplexer with the parameters calculated before. It is necessary to ensure that the center wavelength of each stage is aligned, which has a great impact on the insertion loss and crosstalk of the device. The simulation result is shown in Figure 3. It can be seen that all channel wavelengths are accurately aligned by the results.

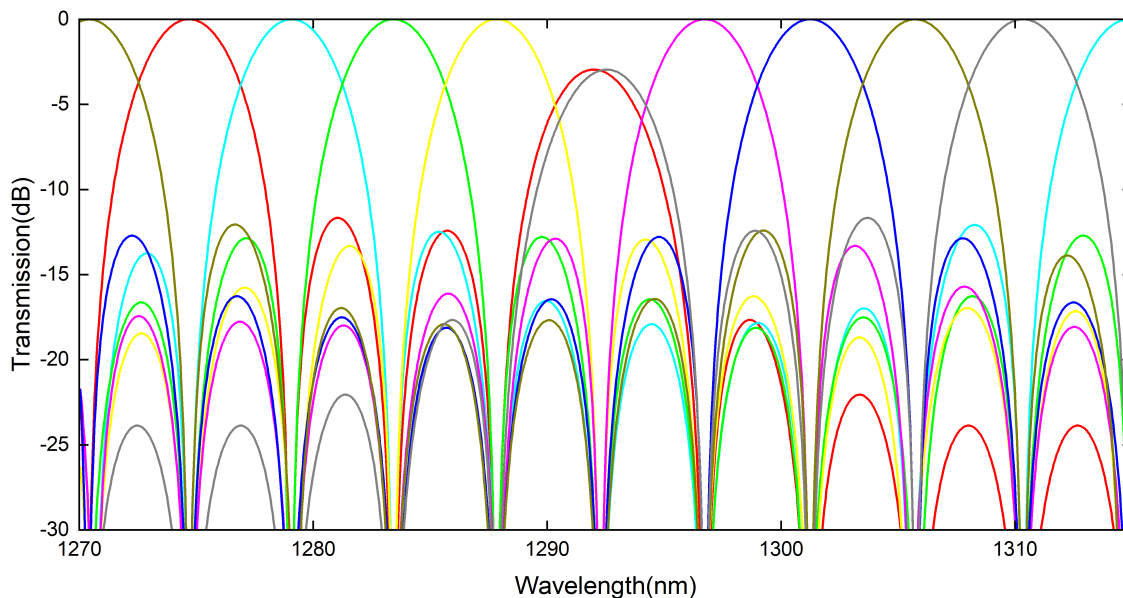
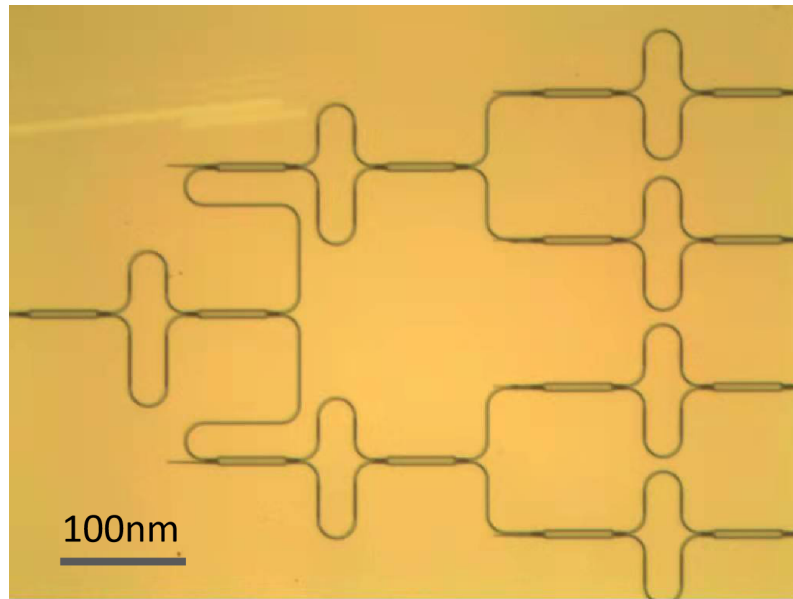


Figure 3. Measured transmission of the 8-channel (de)multiplexer.

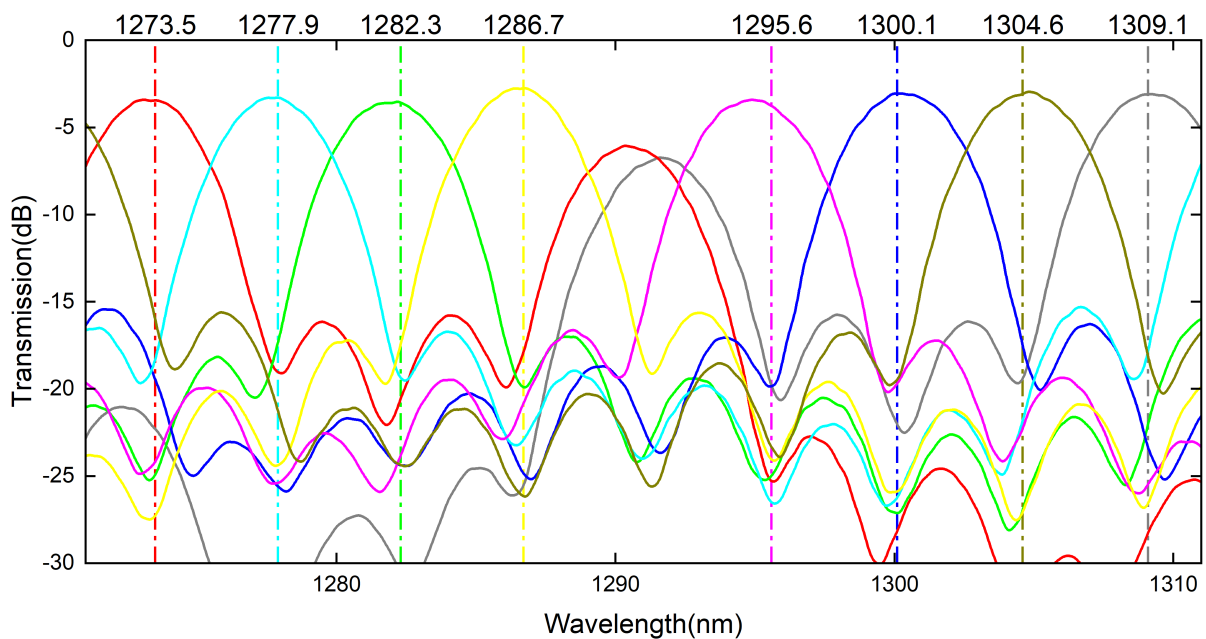
### 3. Device Characterization

Figure 4 shows the micrograph of the fabricated device with a footprint of  $650 \mu\text{m} \times 470 \mu\text{m}$ . An 8-inch silicon-on-insulator wafer with a 220-nm-thick top silicon layer and a 2000-nm-thick buried silicon dioxide layer is used to fabricate the device. The patterns are defined by 193 nm deep ultraviolet photolithography. Inductively coupled plasma etching is employed to fully etch the silicon top layer. A 2000-nm-thick silicon dioxide layer is deposited on the silicon layer by plasma-enhanced chemical vapor deposition (PECVD).



**Figure 4.** The microscope images of the fabricated 8-channel LAN WDM (de)multiplexer.

A broadband amplified spontaneous emission (ASE) source and an optical spectrum analyzer (OSA) were used to characterize the fabricated device. The light coupling from ASE to chip and from chip to OSA is edge coupling, and then the coupling loss is eliminated from the test results by normalization. Figure 5 plots the measured transmission spectra at all eight outputs of the device. The measurement results indicate that the eight-channel central wavelengths are well aligned to the standard wavelength range. The IL of the central wavelength varies between 2.77 dB and 3.77 dB. Higher insertion loss is mainly caused by the following reasons. The first reason is that MMI has a large insert loss. According to our measurement, the loss of each MMI is approximately 0.4 dB. In future work, we plan to use bent directional couplers to reduce the loss and footprint while ensuring broadband characteristics [20,21]. The deviation of the center wavelength of the device will also introduce additional loss. As can be seen from Figure 5, the deviation of ch6 is 0.7 nm (1294.9 nm to 1295.6 nm), which introduces 0.4 dB loss at the standard center wavelength. More detailed test results are shown in Table 3.



**Figure 5.** Measured transmission of the 8-channel (de)multiplexer.

**Table 3.** Performance of the 8-channel (de)multiplexer.

Lane	Ch1	Ch2	Ch3	Ch4
IL(dB)	-3.45	-3.30	-3.57	-2.77
Crosstalk (dB)	-12.54	-14.13	-13.91	-15.15
Deviation (nm)	-0.4	0	-0.1	+0.06
Lane	Ch6	Ch7	Ch8	Ch9
IL (dB)	-3.77	-3.06	-3.08	-3.10
Crosstalk (dB)	-16.08	-16.42	-14.43	-15.06
Deviation (nm)	-0.7	+0.08	+0.23	+0.1

To evaluate inter-die distribution, the measured spectra for all output channels located in five different areas across the 8-inch wafer were superimposed, as shown in Figure 6. Figure 7 shows the superimposed results of the 8-channel spectra and each color represents the test results of a chip, and the statistical distribution in terms of insertion loss and deviation for all channels is shown in Table 4. It can be seen that the range of changes in loss is large, which may be due to coupling errors. The average insertion loss of all channels is 2.8 dB, which is mainly caused by the loss of MMI, and is consistent with our previous test results. The center wavelength of each channel is within the specified wavelength, and the deviation of each channel is less than 1 nm. This proves the reproducibility and fabrication tolerance of our device. At the same time, the small device footprint means that it is easy to integrate with other devices. These features demonstrate that our device has broad prospects in the application of 400GbE silicon optical modules.

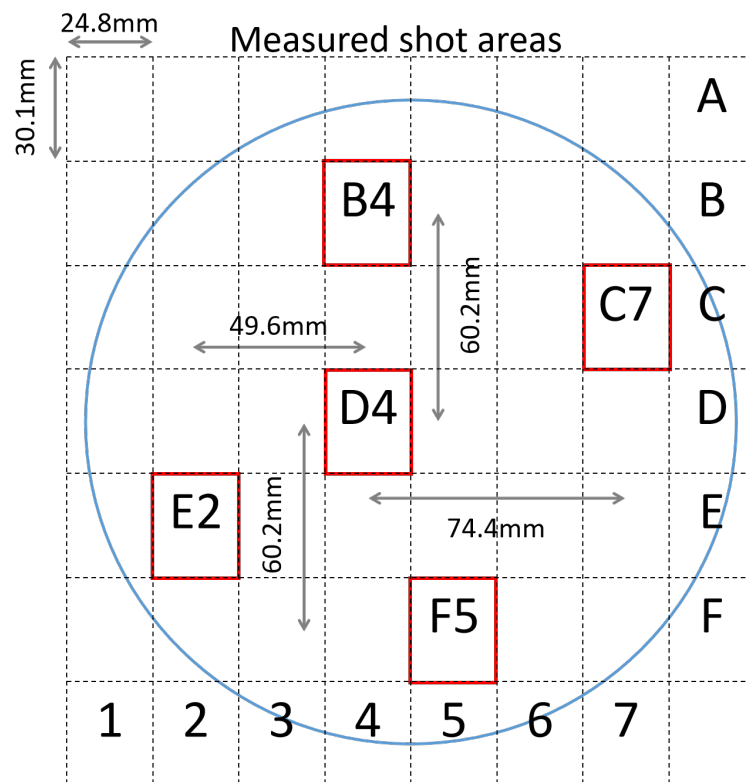


**Figure 6.** Diagrams of an 8-inch SOI wafer and the locations of five devices under test.

**Table 4.** Statistical distribution in terms of insertion loss and deviation for all channels.

Lane	IL (dB)	Deviation (nm)	Lane	IL (dB)	Deviation (nm)
Ch1	$-3.25 \pm 0.57$	$-0.4 \sim +0.13$	Ch6	$-2.56 \pm 0.5$	$-0.07 \sim +0.12$
Ch2	$-2.88 \pm 0.42$	$-0.32 \sim -0.05$	Ch7	$-2.60 \pm 0.55$	$-0.04 \sim +0.01$
Ch3	$-3.13 \pm 0.79$	$-0.52 \sim +0.05$	Ch8	$-2.75 \pm 0.4$	$-0.59 \sim +0.32$
Ch4	$-2.61 \pm 0.44$	$-0.28 \sim +0.06$	Ch9	$-2.88 \pm 0.8$	$-0.02 \sim +0.14$

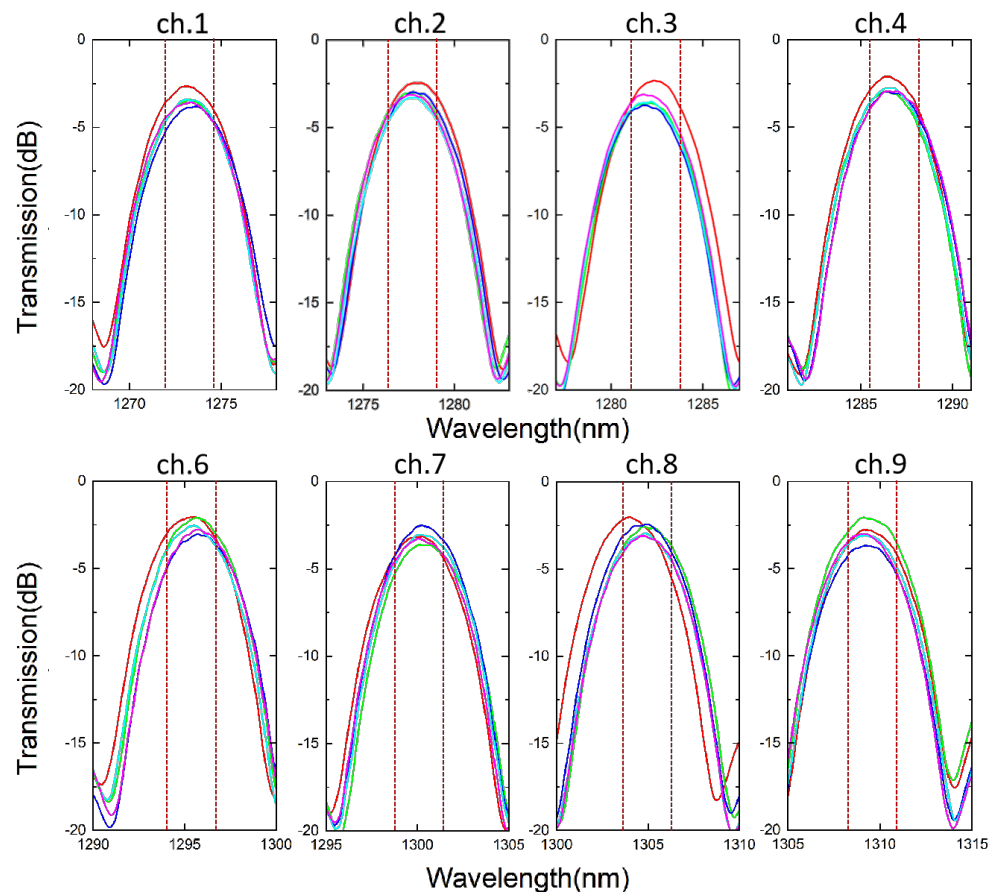


**Figure 7.** Measured transmission of five 8-channel (de)multiplexer across an 8-inch wafer. The range between the red dotted lines is the wavelength range of each channel.

#### 4. Conclusions

In conclusion, we have theoretically and experimentally demonstrated an 8-channel LAN WDM (de)multiplexer based on the cascaded MZIs, which is designed for the 400GBASE-FR8 and 400GBASE-LR8 norm. The eight-channel central wavelengths of this device are accurately aligned with the target wavelength range. Five multiplexers are characterized with the superimposed transmission spectra to prove the reproducibility and fabrication tolerance. The measurement results show that the insertion loss of each channel is approximately 2.8 dB, and the deviation is less than 1 nm. All these features make our proposed (de)multiplexer promising for 400GBASE-FR8 and 400GBASE-LR8 applications.

**Author Contributions:** Conceptualization, Z.Z.; funding acquisition, X.F. and L.Y.; methodology, Z.Z. and H.C.; software, Z.L. and G.Z.; supervision, L.Y.; validation, H.C.; visualization, Z.Z. and J.N.; writing—original draft, Z.Z.; writing—review and editing, Z.Z. and J.N. All authors have read and agreed to the published version of the manuscript.

**Funding:** This research was funded by the National Key Research and Development Program of China (2017YFA0206402), National Science Fund for Distinguished Young Scholars (61825504) and National Natural Science Foundation of China (61975198).

**Data Availability Statement:** Not applicable.

**Conflicts of Interest:** The authors declare no conflicts of interest.

### Abbreviations

The following abbreviations are used in this manuscript:

MZI	Mach–Zehnder interferometer
LAN	Local Area Network
WDM	Wavelength Division Multiplexing
MMI	multi-mode interference
AWG	arrayed-waveguide grating
EDG	echelle diffraction grating
CWDM	Coarse Wavelength Division Multiplexing
SiN	silicon nitride
PSR	polarization splitter rotator
FDE	finite-difference eigenmode
EME	eigenmode expansion
IL	insertion loss
PECVD	plasma-enhanced chemical vapor deposition
ASE	amplified spontaneous emission
OSA	optical spectrum analyzer

### References

- Brackett, C.A. Dense wavelength division multiplexing networks—Principles and applications. *IEEE J. Sel. Areas Commun.* **1990**, *8*, 948–964. [CrossRef]
- 200 Gb/s and 400 Gb/s Ethernet Task Force. Available online: <http://www.ieee802.org/3/bs/> (accessed on 20 October 2021).
- Akca, B.I.; Doerr, C.R.; Sengo, G.; Worhoff, K.; Pollnau, M.; de Ridder, R.M. Broad-spectral-range synchronized flat-top arrayed-waveguide grating applied in a 225-channel cascaded spectrometer. *Opt Express* **2012**, *20*, 18313–18318. [CrossRef] [PubMed]
- Pathak, S.; Vanslebrouck, M.; Dumon, P.; Thourhout, D.V.; Bogaerts, W. Optimized Silicon AWG With Flattened Spectral Response Using an MMI Aperture. *J. Lightwave. Technol.* **2013**, *31*, 87–93. [CrossRef]
- Shi, W.; Yun, H.; Lin, C.; Greenberg, M.; Wang, X.; Wang, Y.; Fard, S.T.; Flueckiger, J.; Jaeger, N.A.F.; Chrostowski, L. Ultra-compact, flat-top demultiplexer using anti-reflection contra-directional couplers for CWDM networks on silicon. *Opt. Express* **2013**, *21*, 6733–6738. [CrossRef] [PubMed]
- Oguma, M.; Kitoh, T.; Shibata, T.; Inoue, Y.; Jinguji, K.; Himeno, A.; Hibino, Y. Four-channel flat-top and low-loss filter for wide passband WDM access network. *Electron. Lett.* **2001**, *37*, 514–515. [CrossRef]
- Horst, F.; Green, W.M.; Assefa, S.; Shank, S.M.; Vlasov, Y.A.; Offrein, B.J. Cascaded Mach-Zehnder wavelength filters in silicon photonics for low loss and flat pass-band WDM (de-)multiplexing. *Opt. Express* **2013**, *21*, 11652–11658. [CrossRef] [PubMed]
- Jeong, S.H.; Shimura, D.; Simoyama, T.; Horikawa, T.; Tanaka, Y.; Morito, K. Si-nanowire-based multistage delayed Mach-Zehnder interferometer optical MUX/DeMUX fabricated by an ArF-immersion lithography process on a 300 mm SOI wafer. *Opt. Lett.* **2014**, *39*, 3702–3705. [CrossRef] [PubMed]
- Tao, S.; Huang, Q.; Zhu, L.; Liu, J.; Zhang, Y.; Huang, Y.; Wang, Y.; Xia, J. Athermal 4-channel (de-)multiplexer in silicon nitride fabricated at low temperature. *Photonics Res.* **2018**, *6*, 686–691. [CrossRef]
- Pan, P.; An, J.; Wang, Y.; Zhang, J.; Wang, L.; Qi, Y.; Han, Q.; Hu, X. Compact 4-channel AWGs for CWDM and LAN WDM in data center monolithic applications. *Opt. Laser Technol.* **2015**, *75*, 177–181. [CrossRef]
- Mikkelsen, J.C.; Bois, A.; Lordello, T.; Mahgerefteh, D.; Menezo, S.; Poon, J.K.S. Polarization-insensitive silicon nitride Mach-Zehnder lattice wavelength demultiplexers for CWDM in the O-band. *Opt. Express* **2018**, *26*, 30076–30084. [CrossRef] [PubMed]
- Xu, H.; Liu, L.; Shi, Y. Polarization-insensitive four-channel coarse wavelength-division (de)multiplexer based on Mach-Zehnder interferometers with bent directional couplers and polarization rotators. *Opt. Lett.* **2018**, *43*, 1483–1486. [CrossRef] [PubMed]
- Xu, H.; Dai, D.; Shi, Y. Low-crosstalk and fabrication-tolerant four-channel CWDM filter based on dispersion-engineered Mach-Zehnder interferometers. *Opt. Express* **2021**, *29*, 20617–20631. [CrossRef] [PubMed]
- Gao, G.; Chen, D.; Tao, S.; Zhang, Y.; Zhu, S.; Xiao, X.; Xia, J. Silicon nitride O-band (de)multiplexers with low thermal sensitivity. *Opt. Express* **2017**, *25*, 12260–12267. [CrossRef] [PubMed]
- Hassan, K.; Sciancalepore, C.; Harduin, J.; Ferrotti, T.; Menezo, S.; Bakir, B.B. Toward athermal silicon-on-insulator (de)multiplexers in the O-band. *Opt. Lett.* **2015**, *40*, 2641–2644. [CrossRef] [PubMed]
- Fujisawa, T.; Takano, J.; Sawada, Y.; Saitoh, K. Low-Loss and Small  $2 \times 4\lambda$  Multiplexers Based on  $2 \times 2$  and  $2 \times 1$  Mach-Zehnder Interferometers With On-Chip Polarization Multiplexing for 400GbE. *J. Lightwave. Technol.* **2021**, *39*, 193–200. [CrossRef]
- Jeong, S.-H. Broadband  $1 \times 8$  channel silicon-nanowire-waveguide WDM filter based on point-symmetric Mach-Zehnder interferometric optical couplers in the O-band spectral regime. *OSA Continuum.* **2019**, *2*, 3564–3575. [CrossRef]

18. Munk, D.; Katzman, M.; Kaganovskii, Y.; Inbar, N.; Misra, A.; Hen, M.; Priel, M.; Feldberg, M.; Tkachev, M.; Bergman, A.; et al. Eight-Channel Silicon-Photonic Wavelength Division Multiplexer With 17 GHz Spacing. *IEEE J. Sel. Top. Quant.* **2019**, *25*, 1–10. [[CrossRef](#)]
19. Jeong, S.-H.; Tanaka, Y. Silicon-wire optical demultiplexers based on multistage delayed Mach-Zehnder interferometers for higher production yield. *Appl. Opt.* **2018**, *57*, 6474–6480. [[CrossRef](#)] [[PubMed](#)]
20. Xu, H.; Shi, Y. Flat-Top CWDM (De)Multiplexer Based on MZI With Bent Directional Couplers. *IEEE Photonics Technol. Lett.* **2018**, *30*, 169–172. [[CrossRef](#)]
21. Chang, L.; Gong, Y.; Liu, L.; Li, Z.; Yu, Y. Low-Loss Broadband Silicon-on-Insulator Demultiplexers in the O -Band. *IEEE Photonics Technol. Lett.* **2017**, *29*, 1237–1240. [[CrossRef](#)]